Stochastic interface dynamics in the Hele-Shaw cell

Oleg Alekseev*
Department of Mathematics and Mechanics, Chebyshev Laboratory, Saint-Petersburg State University, 14th Line, 29b, 199178 Saint-Petersburg, Russia

(Received 5 July 2018; revised manuscript received 25 February 2019; published 22 July 2019)

A one-parametric stochastic regularized dynamics of the interface in the Hele-Shaw cell is introduced. The short-distance regularization suggested by the aggregation model stabilizes the growth by preventing the formation of cusps at the interface and makes the interface dynamics chaotic. The introduced stochastic growth process generates universal complex patterns with the well-developed fjords of oil separating the fingers of water. In a long time asymptotic, by coupling a conformal field theory to the stochastic growth process, we introduce a set of observables (the martingales), whose expectation values are constant in time. The martingales are closely connected to degenerate representations of the Virasoro algebra and can be written in terms of conformal correlation functions. A direct link between Laplacian growth and conformal Liouville field theory with the central charge $c \geqslant 25$ is proposed.

DOI: 10.1103/PhysRevE.100.012130

I. INTRODUCTION

Nonlinear growth phenomena still pose great challenges in nonequilibrium statistical physics and mathematics. The growth processes observed in various physical, chemical, and biological systems typically lead to the formation of self-similar patterns with remarkable geometrical properties [1,2]. Most of them fall naturally into universality classes depending on the mechanism driving the growth. However, even the problems from the same class often require absolutely different approaches.

The relevant examples are the *deterministic* dynamics of the oil/water interface in the Hele-Shaw cell [3] and discrete *stochastic* fractal growth, such as diffusion-limited aggregation (DLA) [4]. Although these phenomena are both diffusion driven growth processes, the stochastic dynamics is mainly studied numerically, whereas the deterministic Hele-Shaw problem is known to possess a real mathematical structure owing to integrability [5,6]. A single framework unifying both processes must resolve the following main obstacles: (1) A naive limit of the vanishing particle size in DLA leads to the ill-defined Hele-Shaw problem when the interface quickly develops cusps, and (2) it is problematic to introduce stochastic interface dynamics in the Hele-Shaw cell because the incompressible viscous fluid prevents *local* fluctuations in pressure.

Both obstacles can be resolved by introducing a short-distance regularization of the Hele-Shaw problem suggested by the aggregation model [7–9]. Namely, one can consider the short-distance cutoff so that the change in areas of domains is quantized and equals an integer multiple of the area quanta $\hbar$. The cutoff prevents the cusps' production and generates inevitable noise (fluctuations) on the microscale (the scale on the order of $\hbar$). The regularization procedure leads to the violation of the incompressibility condition on the microscale. Thus, it becomes possible to introduce *local* fluctuations of pressure in the vicinity of the interface, which are forbidden in the idealized (without a surface tension) Hele-Shaw problem. The dissipation of fluctuations with time results in the formation of patterns with the well-developed fjords of oil separating the fingers of water [9].

In this paper, we continue to study the short-distance regularization of the Hele-Shaw problem introduced in Refs. [8,9]. The laboratory observations of the Hele-Shaw flow show the formation of multifingered branched universal patterns. Remarkably, these patterns are known to be (mono)fractals with the numerically obtained Hausdorff dimension $D_h = 1.71 \pm 0.01$, which appears to be robust and universal [10]. The conventional *analytical* methods to study Laplacian growth, inspired by the Riemann mapping theorem, usually far from making the problem of multifractal analysis tractable. Although some solutions of the idealized Laplacian growth problem are found to be in good agreement with experiments [11], they cannot explain the fractal structure of the interface. Thus, our goal is to introduce a system of coupled stochastic partial differential equations [see Eqs. (1), (2), and (4) below], which generates stochastic interface dynamics in the Hele-Shaw cell and results in the formation of fractal patterns.

The structure of this paper is straightforward: After recalling the Laplacian growth problem regularized by the short-distance cutoff, we introduce a model for stochastic interface dynamics in the Hele-Shaw cell and report a family of martingales, which can be expressed in terms of the correlation functions of the conformal field theory (CFT) with the central charge $c \geqslant 25$. Afterwards, we perform numerical simulations with which we analyze the patterns, generated by the model. Finally, we draw our conclusions and indicate some open problems.

*teknoanarchy@gmail.com

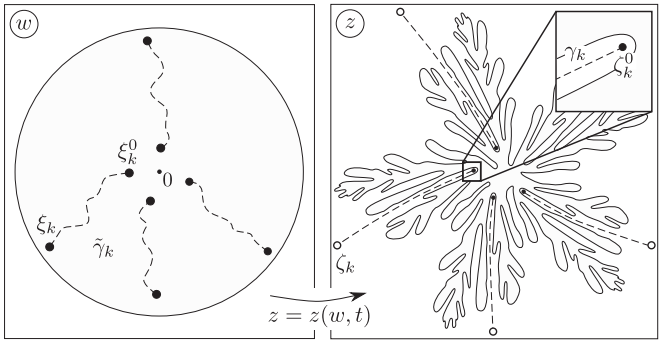

FIG. 1. The time-dependent conformal map $z(w,t)$ from the complement of the unit disk $\mathbb{D}^+$ on the auxiliary w plane to the exterior of the domain D_t^+ on the z plane. The dashed lines on the z plane represent the fjord centerlines γ_k bounded by the end points $\zeta_k^0 \equiv z[1/\bar{\xi}_k^0(t), t] = \text{const}$ and $\zeta_k = z[1/\bar{\xi}_k(t), t]$. The curve $\tilde{\gamma}_k$ on the w plane with the end points ξ_k and ξ_k^0 is the image of γ_k under the conformal map.

II. A SHORT-DISTANCE REGULARIZATION OF LAPLACIAN GROWTH

The *Loewner-Kufarev approach* is a convenient method to study the interface dynamics in the Hele-Shaw cell [12,13]. Let $z(w,t)\colon \mathbb{C}\setminus\mathbb{D}^+ \to \mathbb{C}\setminus D_t^+$ be the time-dependent conformal map from the exterior of the unit disk $\mathbb{D}^+$ on the auxiliary w plane to the exterior of the simply connected domain D_t^+ on the z plane (see Fig. 1). The exterior of the droplet $\mathbb{C}\setminus D_t^+$ will be called D_t for brevity. The map is unique provided the following conditions: $z(\infty,t)=\infty$, and the conformal radius $r(t)=z'(\infty,t)$ is a positive function of time t. Then, the growth of D_t^+ can be represented as a Loewner chain, i.e., a sequence of conformal maps satisfying the following partial integrodifferential equation[1] [12,13]:

$$\dot{z}(w,t) = -wz'(w,t)\int_0^{2\pi}\frac{d\phi}{2\pi}\frac{e^{i\phi}+w}{e^{i\phi}-w}\rho(e^{i\phi},t), \qquad (1)$$

where $z(w,0)=w$, and the function $\rho(w,t)$ is the Loewner density. If $\rho(e^{i\phi},t)=\delta(e^{i\phi}-e^{i\phi_0})$ is a Dirac peak at the point $e^{i\phi_0}$, Eq. (1) generates a *local* Loewner growth [12]; stochastic dynamics of the peak at the unit circle leads to the famous Schramm-Loewner evolution (SLE) [14]. In the case of *nonlocal* growth processes, the density is a smooth function on the unit circle. It determines the normal velocity of the boundary,[2] $v_n = |z'|^{-1}\,\mathrm{Im}(\bar{z}_t z_\phi)$ as follows: $v_n(e^{i\phi},t) = |z'(e^{i\phi},t)|\rho(e^{i\phi},t)$. In particular, the *idealized* (without a surface tension) deterministic Laplacian growth is generated by the density $\rho(e^{i\phi},t)=Q/|z'(e^{i\phi},t)|^2$, where Q is the growth rate. We briefly recall the main features of the idealized Laplacian growth problem in Appendix A.

The short-distance regularization of Laplacian growth implies the existence of the dimensional cutoff $\hbar$, i.e., the minimal value (quanta) of the change in the area of the water region allowed in the model. Under these circumstances, the interface dynamics in the Hele-Shaw cell is described by the Loewner chain (1) with the following Loewner density [9] (see also Appendix A):

$$\rho(w,t) = \frac{1}{|z'(w,t)|^2}\left[Q - 2\nu\sum_{k=1}^{N}\mathrm{Re}\,\frac{\xi_k(t)}{w-\xi_k(t)}\right], \qquad (2)$$

where $\nu=\hbar/\delta t$ is the cutoff of the growth rate Q ($\nu \ll Q$),[3] and the collective coordinates $\xi_k(t)$ on the w plane $|\xi_k|<1$ parametrize "slow" fluctuations of the interface velocity obtained by averaging over the "fast" ones. In Ref. [9], it was shown that dissipation of fluctuations with time, generated by Dyson Brownian motion, results in the Calogero-type dynamics of the coordinates,

$$\frac{d\xi_k}{\xi_k} = -\sigma\, d\tau(t) + \frac{1}{2}\sum_{l\neq k}^{N}\frac{\xi_k+\xi_l}{\xi_k-\xi_l}d\tau(t), \qquad (3)$$

where the constant $\sigma = Q/\nu$ produces a drift of ξ_k's toward the origin and the "auxiliary time" $\tau(t)$ parametrizes the motion of poles inside the unit disk.

In Appendix B, we briefly review the growth process determined by the set of coupled Eqs. (1)–(3). We also argue that the patterns generated by these equations capture the main geometrical features of the patterns typically observed in experiments [15,16]. However, the quantitative analysis of the solutions requires to establish an exact relation between the auxiliary and the physical times.

III. STOCHASTIC LAPLACIAN GROWTH

In this section, we propose a model for stochastic interface dynamics in the Hele-Shaw cell, which makes the experimentally observed patterns more amenable to an exact *analytic* treatment. We introduce stochastic dynamics by adding noise to the motion of the poles $\xi_k(t)$ of the Loewner density (2). The corresponding (random) curves on the z plane $\zeta_k(t) = z[1/\bar{\xi}_k(t), t]$ are the centerlines of the fjords of oil[4] separating the fingers of water[5] (see Fig. 1). Thus, we consider each fjord as the result of stochastic evolution.

A statistical theory of stochastic Laplacian growth studies possible outcomes of the growth process when the initial pattern is known. One can argue that the formation of viscous fingers is described by the relaxation to equilibrium in the weakly nonequilibrium statistical system [9]. This observation yields a striking conclusion that *in the long time asymptotic* the statistical weights of patterns should obey the ordinary Gibbs-Boltzmann distribution, which, as a rule, is not applied out from equilibrium.

The partition function for the system Z_{D_0} is given by the sum of Boltzmann weights $\mathcal{F}_{D_t}$ for the possible outcomes D_t of the growth process $D_0 \to D_t$, $(t \gg t_0)$, provided the initial

[1] Here and below, the primes and dots denote partial derivatives with respect to the coordinate and time, respectively.

[2] In what follows, the bar denotes complex conjugation.

[3] One can ignore the details of the construction and consider the cutoff ν as the independent parameter of the model (instead of $\hbar$), which appears explicitly in subsequent calculations, and determines the minimal allowed value of the growth rate.

[4] The centerlines are equidistant from the fjord's edges.

[5] See Ref. [9] and Appendices B and C for a brief review.

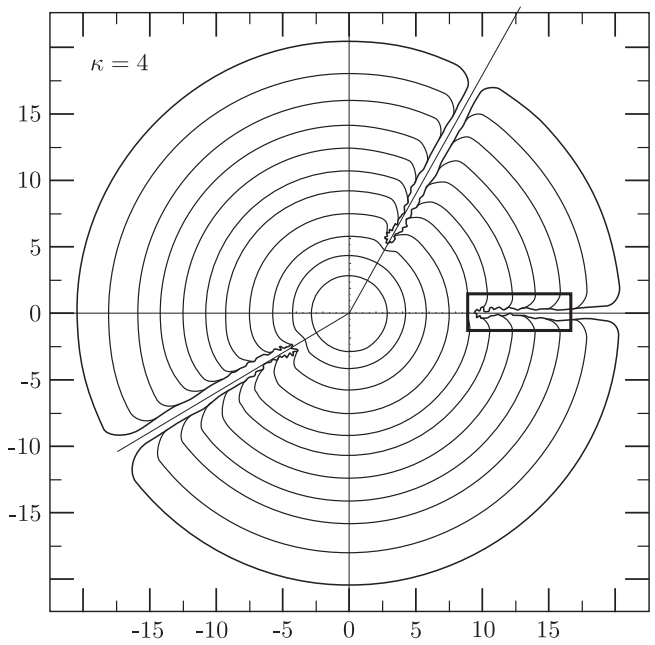

FIG. 2. We plot the interfaces $y = \mathrm{Im}\, z(e^{i\phi}, t)$ vs $x = \mathrm{Re}\, z(e^{i\phi}, t)$ at an increasing time sequence at κ. The interface develops three fjords directed along the radial lines. The bottoms of the fjords at the points $\zeta_1^0 = 10$, $\zeta_2^0 = 3.21 + 5.96i$, and $\zeta_3^0 = -4.61 - 3.07i$ are the stagnation points of the interface dynamics. On the large scale, the fjords closely resemble the ordinary U-shaped fjords with parallel walls, which can be nicely approximated by the smooth logarithmic solutions of the idealized Laplacian growth problem [24]. However, one can note irregularity of the interface at the bottoms of the fjords. The black box shows the region in the bottom of the fjord $\zeta_1^0 = 10$, which is further enlarged in Figs. 3 and 4.

pattern D_0 is given.[6] Remarkably, in the long time asymptotic, the Boltzmann weights can be identified with the martingales[7] of the stochastic growth process (cf. Refs. [18,19]). Below, we show that the patterns D_t possess deep fjords starting at the "stagnation points" (points of the interface that stay almost fixed during growth) and going toward infinity (see Fig. 2) as $t \to \infty$. The positions of stagnation points are specified by the initial domain D_0, whereas the shapes of fjords vary from sample to sample. Thus, the Boltzmann weights $\mathcal{F}_{D_t}$ depend on the position of the fjords and can be written in terms of certain correlation functions (7).

The construction of martingales of stochastic Laplacian growth leads to the following *proposition*:

Let us consider the interface dynamics in the Hele-Shaw cell, generated by the Loewner chain (1) with the density (2) so that the poles $\xi_k(t)$ of the density move stochastically with time. Then, the resulting interface dynamics is stochastic and, moreover, possesses a set of statistical martingales in the long time asymptotic [which are identified with the statistical weights (7) of patterns], provided the random processes $\xi_k(t)$ satisfy the following system of coupled stochastic differential equations:[8]

$$d\,\ln\,\xi_k = -\sigma\, dq_k - \frac{\kappa}{2} g_k(\xi_1, \ldots, \bar{\xi}_1, \ldots) dq_k + \frac{1}{2}{\sum_{l=1}^{N}}' \left(\frac{\xi_k + \xi_l}{\xi_k - \xi_l} + \frac{\xi_k + 1/\bar{\xi}_l}{\xi_k - 1/\bar{\xi}_l} \right) dq_k + i\, dW_k(q_k), \tag{4}$$

with the initial conditions $\xi_k(t_0) = \xi_k^0$, which determine the initially perturbed pattern D_0.

The driving terms $W_k(q_k) = \sqrt{\kappa/2} B_k(q_k)$ in Eq. (4) are proportional to the uncorrelated Brownian motions $B_k(q_k)$ with the mean zero and covariance $\mathrm{cov}[B_k(q_k) B_s(q_s')] = \delta_{ks} \min(q_k, q_k')$, where the ordinary time variable t is replaced by the auxiliary times $q_k(t)$, expressed by

$$dq_k(t) = \nu |z'(1/\bar{\xi}_k^0(t), t)|^{-2} dt. \tag{5}$$

The time evolution of the points $\xi_k^0(t)$, generated by the stochastic Loewner chain, Eqs. (1), (2), and (4), will be discussed below [see Eq. (14)]. Note that there was only one auxiliary time in Eq. (3), obtained on the assumption of dissipation of fluctuations at the interface with time [9]. However, this qualitative consideration fails to specify an explicit relation between the auxiliary and the physical times. A more systematic analysis of the problem, presented hereafter, shows that more than one auxiliary time $q_k(t)$ individually parametrizing the fjords evolution, are required to simulate the growth process properly (cf. Ref. [18] where the multiple SLE curves are parametrized by multiple times).

The diffusion constant $\kappa > 0$ measures the noise strength $\mathrm{cov}[W_k(q_k) W_s(q_s')] = (\kappa/2)\delta_{ks} \min(q_k, q_k')$ and labels a continuous family of stochastic Laplacian growth processes. We argue below, that multifractal properties of grown patterns depend on the value of κ.

The function $g_k = \xi_k^{-1}(\xi_k \partial_{\xi_k} + \bar{\xi}_k \partial_{\bar{\xi}_k}) \ln Z$ in Eq. (4) is the logarithmic derivative of the correlation function $Z = \langle \prod_k \Psi(\xi_k, \bar{\xi}_k) \rangle_{\mathbb{D}}$ of the primary fields Ψ with the conformal dimensions $h = -(6+\kappa)/(2\kappa)$ of the boundary CFT with the central charge $c = 1 + 3(\kappa+4)^2/(2\kappa)$. We briefly recall the basics of CFT below.

In the next section, we argue that the system of coupled stochastic equations, (1), (2), and (4) admits a set of martingales $\mathcal{F}_{D_t}$, which is closely connected to the conformal correlation functions as shown below (7). We will follow the guideline of Ref. [18] where the construction of martingales associated with interfaces was proposed. The main idea is to couple a critical statistical system to the exterior of the growing domain D_t and consider the observables of the system, i.e., the correlation functions of local operators. By conditioning these observables to be the martingales of stochastic interface dynamics, one puts strong constraints on the motion of the poles $\xi_k(t)$ and auxiliary times $q_k(t)$.

[6] In Fig. 2, we show a particular outcome of stochastic growth of the initially perturbed unit circle. It is clear that one has infinitely many outcomes for the same initial interface.

[7] Roughly speaking, the martingales are the stochastic processes, whose expectation values are constant in time [17].

[8] The primed sum means that the singular term is excluded.

IV. MARTINGALES OF STOCHASTIC INTERFACE DYNAMICS

Our analysis is based on the methods inspired by conformal field theory. Therefore, it is instructive to begin this section by recalling the basics of CFT. Let us consider a CFT in the external domain D_t. It is characterized by the set of scaling operators (primary fields) $\Phi_h(z,\bar z)$ constituting representations of the Virasoro algebra [20,21]. A set of conformal dimensions h specifies the transformation of correlation functions of primary fields under conformal maps,[9]

$$\left\langle \prod_{k=1}^{N} \Phi_{h_k}(z_k,\bar z_k) \right\rangle_{D_t} = \left\langle \prod_{k=1}^{N} |w'(z_k,t)|^{2h_k} \Phi_{h_k}(w_k,\bar w_k) \right\rangle_{\mathbb{D}}. \quad (6)$$

The correlation functions are known to be closely connected to SLE statistical martingales [22]. A similar approach can be used in the case of stochastic Laplacian growth provided considerably strict constraints. Let us introduce the following normalized correlation function,

$$\mathcal{F}_{D_t}(\{\zeta,\zeta^0\}) = \frac{\left\langle \prod_k \Psi(\zeta_k,\bar\zeta_k)\Phi_h(\zeta_k^0,\bar\zeta_k^0)\right\rangle_{D_t}}{\left\langle \prod_k \Psi(\zeta_k,\bar\zeta_k)\right\rangle_{D_t}}, \quad (7)$$

where $k=1,\dots,N$. The positions of the fields are specified by the end points $\zeta_k^0 \equiv \zeta_k(t_0) = \text{const}$ and $\zeta_k \equiv \zeta_k(t)$ of the dynamically generated centerlines of the fjords of oil that separate fingers of water (see Fig. 1),

$$\zeta_k^0 = z[1/\bar\xi_k^0(t),t] = \text{const}, \quad \zeta_k(t) = z[1/\bar\xi_k(t),t]. \quad (8)$$

The relation between the singularities of the conformal map and the positions of fjords can be established by using the Schwarz function approach [11,23].

Stochastic evolution of the domain D_t results in the Langevin dynamics of the correlation functions, which can be conventionally studied by mapping (7) to the w plane by means of (6),

$$\mathcal{F}_{D_t}(\{\zeta,\zeta^0\}) = \mathcal{F}_{\mathbb{D}}(\{w,w^0\}) \prod_{k=1}^{N} |w'(\zeta_k^0,t)|^{2h_k}, \quad (9)$$

where $w_k(t) = 1/\bar\xi_k(t)$ and $w_k^0(t) = 1/\bar\xi_k^0(t)$.

The time evolution of the inverse map $w = z^{-1}$ can be obtained from Eq. (1) by the method of characteristics,

$$\frac{dw(z,t)}{dt} = w(z,t)\int_0^{2\pi} \frac{d\phi}{2\pi} \frac{e^{i\phi}+w(z,t)}{e^{i\phi}-w(z,t)} \rho(e^{i\phi},t), \quad (10)$$

with the initial condition $w(z,0)=z$. Let $w \to w+\epsilon(w)$ be the infinitesimal conformal transformation generated by the Loewner chain (10), i.e., $\epsilon(w) = wp(w)dt$, where $p(w)$ denotes the integral over the angle in Eq. (10). Since $\mathrm{Re}\, p(e^{i\phi}) < 0$, this *transformation does not preserve the geometry*.[10] Taking account of $\epsilon(w)/w = \bar w \epsilon(1/\bar w)$ when $|w| = 1$ and $p(1/\bar w) = -\bar p(\bar w)$, one determines the transformation of the antiholomorphic sector in the vicinity of the unit circle: $\bar w \to \bar w - \bar\epsilon(\bar w)$.

Since the conformal map changes with time stochastically, we take the Itô derivative of Eq. (9). To begin with, let us consider a variation of the primary field $d\Phi_h = |w'(z,t)|^{2h}(h\epsilon' - h\overline{\epsilon'} + \epsilon\partial_w - \bar\epsilon\partial_{\bar w})\Phi_h$. Below, only the key points of the computation will be mentioned whereas the technical details will be presented elsewhere.

Conformal transformations at the bottoms of fjords. First, if point w is located in the vicinity of the unit circle, i.e., $w \approx e^{i\theta}$, the difference $I(w) = wp'(w) - \overline{wp'(w)}$ reduces to the contour integral around this point,

$$I(w) = -2w \oint_w \frac{du}{2\pi i} \frac{\rho(u,t)}{(u-w)^2}. \quad (11)$$

Since $\rho(u,t)$ depends on the conformal map, critical points of $z'(w,t)$ contribute to the integral. The map $z(w,t)$ is conformal outside the unit disk so that all singularities of $z'(w,t)$ are located inside.

It is convenient to consider the growth process, specified by Eqs. (1), (2), and (4) in the discrete framework. Then, $z'(w,t_i)$ can be written in the form [9]

$$z'(w,t_i) = r(t_i) + \sum_{k=1}^{N}\sum_{j=0}^{i} \frac{\bar c_{k,j}}{w-\xi_k^j(t_i)}, \quad (12)$$

where $\xi_k^j(t_i)$ is the position of the jth point of the cut $\tilde\gamma_k(t_i)$ of the map $z(w,t_i)$. The coefficients $c_{k,j}$ are the stochastic variables, determined by displacements of the images of the points ξ_k^j on the z plane per time unit [9],

$$c_{k,j} = \nu\,\Delta t\left(\frac{1}{\Delta\zeta_k(t_j)} - \frac{1}{\Delta\zeta_k(t_{j-1})}\right), \quad (13)$$

where $\Delta\zeta_k(t_j) = \zeta_k(t_j) - \zeta_k(t_{j-1})$. Contrary to idealized Laplacian growth, the interface evolution, (1), (2), and (4), does not preserve the number of singular points. At each time unit Δt, the function $z'(w,t_i)$ develops N new poles[11] at the points $\xi_k(t_i) \equiv \xi_k^i(t_i)$ determined by the stochastic dynamics (4).

The dynamics of the poles $\xi_k^j(t)$ of $z'(w,t)$ is governed by the constants of motion [9] (see also Appendix C),

$$\zeta_k(t_j) = z[1/\bar\xi_k^j(t_i),t_i] = \text{const} \quad (j<i), \quad (14)$$

and $2\pi t_i = (1/2i)\oint_{|w|=1} \overline{z(w,t_i)} z'(w,t_i)dw$ is the area of the domain at time t_i. The positions of the remaining N poles $\xi_k^i(t_i)$ are determined by the stochastic differential equation (4). Thus, the system of coupled equations (1), (2), and (4) is self-consistent and determines uniquely the interface dynamics by specifying the positions of critical points of the conformal map.

In the asymptotic $r(t) \to \infty$ (i.e., as $t \to \infty$), the poles $\xi_k^0(t)$ approach the unit circle $\ln[1-|\xi_k^0(t)|] \approx -r(t)/|\alpha_k|$ where the constants α_k are related to the widths of the

[9] We only consider the spinless operators with equal holomorphic and antiholomorphic conformal dimensions.

[10] More precisely, the CFT is defined on the Schottky double of the viscous fluid domain D_t.

[11] In the limit $\Delta t \to 0$, the generation of poles results in the evolution of the branch cuts of $z'(w,t)$.

fjords [24]. The roots $u_k^j(t)$ and poles $\xi_k^j(t)$ of the function (12) are separated in pairs so that $|u_k^j(t)-\xi_k^j(t)|\sim 1/r(t)$. Therefore, the contribution of the factor $|z'(w,t)|^{-2}$ to the integral (11), namely, $-2\,\mathrm{Im}[w_k^0 z''(w_k^0)/z'(w_k^0)]\rho(w_k^0)\sim \rho(w_k^0)/r(t)$ is suppressed when compared to the contribution of the poles at $w=\xi_k$ of the density (2). Thus,

$$I(w_k^0)=\frac{-2\nu}{|z'(w_k^0,t)|^2}\sum_{j=1}^{N}\left[\frac{w_k^0\xi_j}{(w_k^0-\xi_j)^2}-\text{c.c.}\right]+O(1/r), \tag{15}$$

where c.c. denotes the complex conjugated terms. The prefactor in Eq. (15) is proportional to the normal interface velocity squared $v_n^*(e^{i\theta},t)=Q|z'(e^{i\theta},t)|^{-1}$. It becomes exponentially small [$\ln|z'(w_k^0,t)|\sim r(t)/|\alpha_k|$] at the bottoms of fjords where interfaces develop stagnation points that stay almost fixed during growth.

Boundary conditions. The second key point in the computation of $d\mathcal{F}$ is the Neumann boundary condition for the fields $\Phi_h(w_k,\bar w_k)=\Phi_h(e^{i\theta_k})$ located exponentially close to the unit circle,

$$\partial_n(w\bar w)^h\Phi_h(w,\bar w)|_{w=\exp(i\theta_k)}=0, \tag{16}$$

where $\partial_n=w\partial_w+\bar w\partial_{\bar w}$ is the normal derivative. Note that, in the coordinates, $w=\exp(ix-y)$, Eq. (16) takes the form $\partial_y\Phi_h(x,y)|_{y=0}=0$.

Transformations of fields. The formulas (11), (15), and (16), together with the equality $\mathrm{Re}(dw/w\,dt)=-\rho(w)$ for $w=\exp(i\theta)$, determine the variation of the field $\Phi_h^w(z,\bar z)\equiv|w'(z,t)|^{2h}\Phi_h(w,\bar w)$ under stochastic Laplacian growth,

$$\frac{d\Phi_h^w(\zeta^0,\bar\zeta^0)}{|w'(\zeta^0,t)|^{2h}dt}=[hI(e^{i\theta})+\rho(e^{i\theta})i\partial_\theta]\Phi_h(e^{i\theta}), \tag{17}$$

where $i\partial_\theta=\bar w\partial_{\bar w}-w\partial_w$ stands for the tangential derivative at the unit circle.

Furthermore, let us consider a contribution of the fields $\Psi(\zeta_k,\bar\zeta_k)$ located at the end points $\zeta_k(t)=z[1/\bar\xi_k(t),t]$ of the fjord's centerlines. Since the Jacobians coming from the transformations of the fields are canceled in the numerator and denominator of the correlation function (9), the Itô derivative of $\Psi(\xi,\bar\xi)$ reads

$$d\Psi=-(\kappa/4)(\xi\partial_\xi+\bar\xi\partial_{\bar\xi})^2\Psi\,dq+\partial_\xi\Psi\,d\xi+\partial_{\bar\xi}\Psi\,d\bar\xi. \tag{18}$$

Langevin dynamics of correlation functions. Finally, one can neglect the difference in the normal interface velocities near stagnation points as $r(t)\to\infty$. Namely, the conformal factors $|w'(\zeta_k^0,t)|$ with $k=1,\dots,N$ are equal up to exponentially small corrections in $r(t)$. Then, by taking account of Eq. (4), one obtains the following expression for the Itô derivative of $\mathcal{F}_{D_t}(\{\zeta,\zeta^0\})$:

$$d\mathcal{F}_{D_t}=\prod_{j=1}^{N}|w'(\zeta_j^0,t)|^{2h_j}\sum_{k=1}^{N}\Big[i\,dW_k\big(l_{-1}^{(k)}+\bar l_{-1}^{(k)}\big)+dq_k\Big(-\frac{\kappa}{4}\big(l_{-1}^{(k)}+\bar l_{-1}^{(k)}\big)^2+l_{-2}^{(k,h)}+\bar l_{-2}^{(k,-h)}\Big)\Big]\mathcal{F}_{\mathbb{D}}, \tag{19}$$

where we used (5), took into account that all dq_k's with $k=1,2\cdots$ are equal in the limit $r(t)\to\infty$, and introduced the following differential operators:

$$\begin{aligned}l_{-1}^{(k)}&=\xi_k\partial_{\xi_k},\\ l_{-2}^{(k,h)}&=-\frac{1}{2}\sum_{j\neq k}\frac{\xi_k+\xi_j}{\xi_k-\xi_j}\xi_j\partial_{\xi_j}+\frac{1}{2}\sum_j\frac{\xi_k+1/\bar\xi_j}{\xi_k-1/\bar\xi_j}\bar\xi_j\partial_{\bar\xi_j}\\ &\quad+\frac{1}{2}\sum_j\frac{\xi_k+e^{i\theta_j}}{\xi_k-e^{i\theta_j}}i\partial_{\theta_j}-\sum_j\frac{2h\xi_k e^{i\theta_j}}{(\xi_k-e^{i\theta_j})^2},\end{aligned} \tag{20}$$

where h is the conformal dimension of Φ_h.

Belavin-Polyakov-Zamolodchikov equations. The primary fields of CFT form the highest weight representations of the Virasoro algebra. These representations are not necessarily irreducible because of the existence of the *null vectors* in the Verma modules. A relevant example is the null vector at the second level of the Verma module, which exists whenever the highest weight of the module h takes a value from the Kac table [20],

$$h=h_{21}=-\frac{6+\kappa}{2\kappa}\ \text{when}\ c=1+3\frac{(\kappa+4)^2}{2\kappa}. \tag{21}$$

We emphasize that the central charge is $c\geqslant 25$ so that the Virasoro algebra is a symmetry algebra of the Liouville field theory [25], whereas, in the SLE case, the central charge is $c\leqslant 1$ [22,26]. The reason is that the differential equations for $d\mathcal{F}$, expressing the decoupling of the null vector, match with the expression on the right hand side of Eq. (19) when $c\geqslant 25$.[12]

The correlation functions that involve degenerate fields (corresponding to the null vectors) satisfy the linear partial differential equations called Belavin-Polyakov-Zamolodchikov equations [20]. In particular, the correlation function (7) with N degenerate fields $\Psi(\zeta_k,\bar\zeta_k)$ satisfies the following N differential equations:

$$\Big[-\frac{\kappa}{4}\big(l_{-1}^{(k)}\big)^2+l_{-2}^{(k,h)}\Big]\mathcal{F}_{\mathbb{D}}=0,\quad k=1,\dots,N, \tag{22}$$

and similar equations hold for the antiholomorphic sector. Equations (22) allow one to recast the Langevein dynamics (19) of $\mathcal{F}$ in the form

$$\frac{d\mathcal{F}_{D_t}(\{\zeta,\zeta^0\})}{\prod_k|w'(\zeta_k^0,t)|^{2h_k}}=\sum_{k=1}^{N}\Big[i\,dW_k\big(l_{-1}^{(k)}+\bar l_{-1}^{(k)}\big)-dq_k\frac{\kappa}{2}\Delta^{(k)}\Big]\mathcal{F}_{\mathbb{D}}, \tag{23}$$

where $\Delta^{(k)}=l_{-1}^{(k)}\bar l_{-1}^{(k)}$ is the Laplace operator.

Martingales of stochastic Laplacian growth. Roughly speaking, martingales are the random processes whose expectation values are constant in time, i.e., they satisfy stochastic differential equations without a drift term [17]. The drift term on the right hand side of Eq. (23) measures the degree to which $\mathcal{F}_{D_t}$ fails to be a martingale (cf. Ref. [27]). If the positions of points $\xi_k(t)$ are determined by the equation

[12]Note that the poles ξ_k in (4) attract each other in the tangential direction, whereas, in the (radial) SLE case, they are repealed.

$\sum_{k=1}^{N} \Delta^{(k)} \mathcal{F}_{\mathbb{D}}(\{\xi, \bar{\xi}, e^{i\theta}\}) = 0$, the function (7) becomes the martingale of stochastic Laplacian growth. Therefore, we argued that stochastic interface dynamics (1), (2), and (4), which describe the evolution of N oil fjords starting from a slightly perturbed initial interface, admits a family of martingales closely connected to conformal correlation functions (7).

Statistical mechanics arguments (see, e.g., Ref. [18]) allows one to relate ratios of conformal correlation functions $\mathcal{F}_{D_t}(\zeta_1, \ldots; \bar{\zeta}_1, \ldots)$ with conditioned expectation values of local operators of statistical systems. In particular, the SLE martingales are essential objects for estimating crossing probabilities of random curves, representing the conditioned correlation functions of statistical systems [18]. A similar interpretation holds (with minor reservations) in the case of stochastic Laplacian growth. Namely, instead of random (multiple) SLE curves, one should consider a family of random centerlines of the fjords. Then, the correlation functions (7) are the probabilities of the fjords centerlines to pass through the marked points $\{\zeta_k^0, \zeta_k(t)\}_{k=1}^N$.

V. NUMERICAL SIMULATIONS

In this section, a set of numerical simulations is presented with which we analyze what kind of patterns the introduced model of stochastic Laplacian growth is supposed to produce. In particular, we will unveil a role of the noise strength κ in the pattern formation process. For this purpose, we simulate the process of the fjords' evolution for the various values of the noise strength κ.

In all cases, we consider a tiny perturbation of the initially unit circle $z(w, t_0) = w$ on the z plane so that $v/Q = 0.04$, $r(t_0) = 1$, and $\xi_1(t_0) = 0.1$, $\xi_2(t_0) = 0.07 + 0.13i$, $\xi_3(t_0) = -0.15 - 0.1i$. In Fig. 2, we plot various snapshots of the physical interface $y = \mathrm{Im}\, z(e^{i\phi}, t)$ vs $x = \mathrm{Re}\, z(e^{i\phi}, t)$ at an increasing time sequence, which reproduce the pattern formation processes (1), (2), and (4) for $\kappa = 4$. One can observe a generation of the pattern with three fjords growing in the radial direction. The tips of the fjords, located at the points $\zeta_1^0 = 10$, $\zeta_2^0 = 3.21 + 5.96i$, and $\zeta_3^0 = -4.61 - 3.07i$ are the stagnation points of the interface, which have been observed previously in numerous experiments and numerical simulations (see, e.g., Ref. [28]). Note that, on the large scale, the interface $z(e^{i\phi}, t)$ can be approximated with the smooth nonsingular exact solutions for the idealized Laplacian growth problem [24]. However, the crucial difference between our results and those of Ref. [24] becomes obvious when one addresses geometrical properties of the fjords on the microscale. In order to illustrate this difference in detail, below, we consider the interface in the vicinity of the tip of the fjord at point $\zeta_1^0 = 10$.

In Fig. 3, we show various snapshots of the fjord's centerline $y = \mathrm{Im}\, z[1/\bar{\xi}_1(t), t]$ vs $x = \mathrm{Re}\, z[1/\bar{\xi}_1(t), t]$ in the vicinity of the points $x = 10$, $y = 0$, generated by stochastic dynamics of the points ξ_k's inside the unit circle (4) for $\kappa = 2$, $\kappa = 4$, $\kappa = 8$, and $\kappa = 16$. We see that the higher the noise strength κ, the greater the angular spread of the points, which determine the centerlines of the fjords when the time step goes to zero $\Delta t \to 0$. Contrary to the logarithmic solutions of the idealized Laplacian growth problem, which describes the formation of smooth fjords with parallel walls,

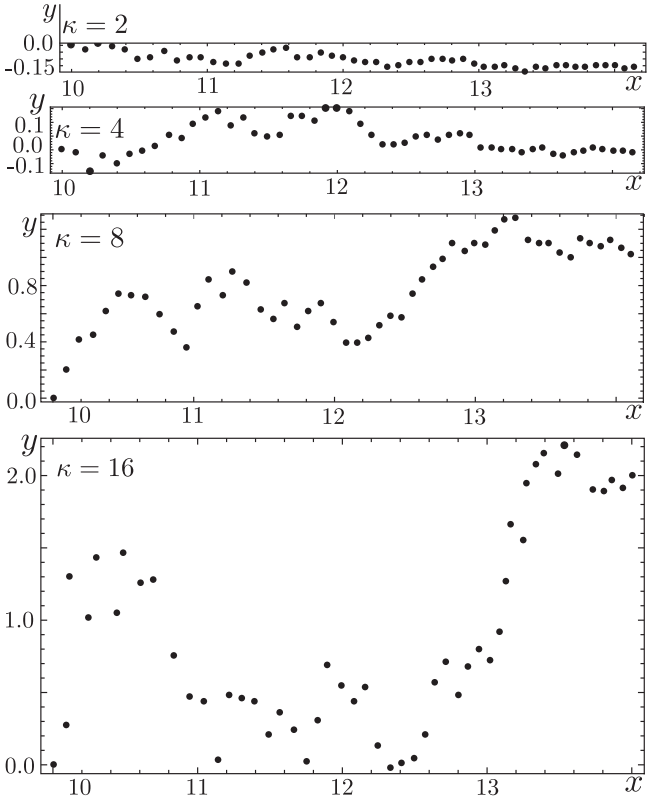

FIG. 3. The boxed region in Fig. 2 is enlarged to reveal a structure of the interface at the bottom of the fjord on the microscale. We plot the fjord's centerlines $y = \mathrm{Im}\, z[1/\bar{\xi}_1(t), t]$ vs $x = \mathrm{Re}\, z[1/\bar{\xi}_1(t), t]$, where $\xi_1(t_0) = 0.1$ in the exterior of the growing domain during the first second of the growth process. The time unit is $\Delta t = 0.01$. The centerlines are generated by stochastic dynamics of singularities of the conformal map (4) for various values of the noise strength $\kappa = 2$, $\kappa = 4$, $\kappa = 8$, and $\kappa = 16$. We see that the higher the noise strength κ, the greater the angular spread of the points along the fjord's centerline. By flowing around these points, the interface develops a fractal structure shown in Fig. 4.

stochastic dynamics results in the formation of fractal patterns at the bottoms of the fjords. However, away from the fjord's tips, the centerlines become almost smooth radial lines, which can be approximated by the logarithmic solutions.

It is remarkable that stochastic dynamics of the poles of the Loewner density (4) results in the formation of variety of tiny fjords on the microscale, which repeatedly merge together to form the larger fjords. We show this feature of the stochastic interface dynamics in Fig. 4 where we have plotted various snapshots of the physical interface $y = \mathrm{Im}\, z(e^{i\phi}, t)$ vs $x = \mathrm{Re}\, z(e^{i\phi}, t)$ near the points $x = 10$, $y = 0$ at times $t = 47$, $t = 50$, $t = 53$, $t = 56$ for two different values of the noise strength $\kappa = 6$ and $\kappa = 16$. The black dots indicate values of the random process $z[1/\bar{\xi}_1(t), t]$ in the first few seconds of the evolution. We see that the positions of the dots can be considered as small obstacles (more precisely, pointlike oil sources as discussed in Appendix B) in the Hele-Shaw flow. By flowing around the obstacles, the interface develops tiny fjords of oil which separate the fingers of water. As follows from Figs. 3 and 4, the higher the noise strength κ, the greater the number of tiny fjords on the microscale at the bottoms of

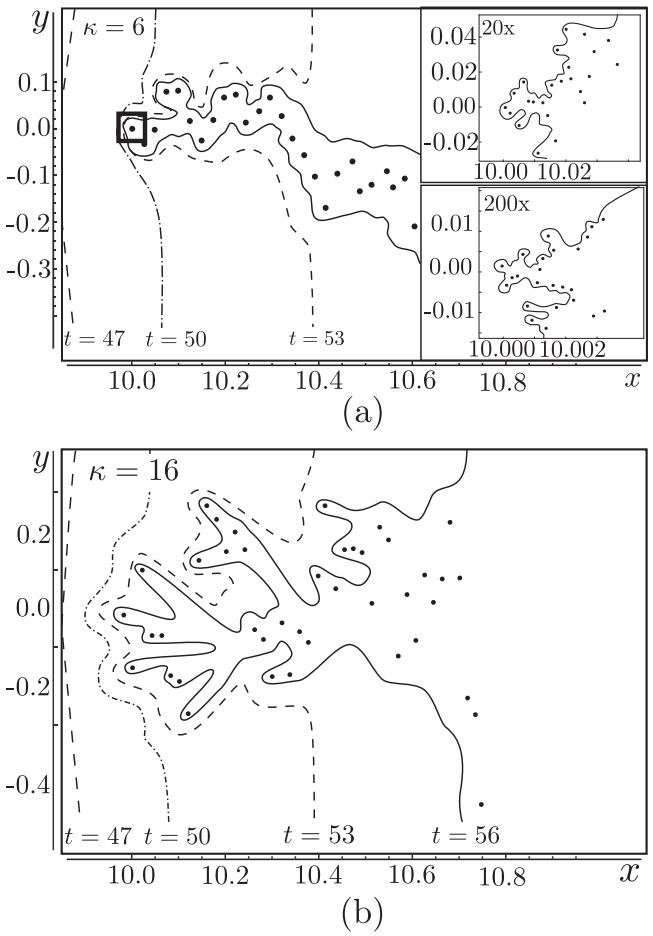

FIG. 4. We plot the interface $y = \mathrm{Im}\, z(e^{i\phi}, t)$ as a function of $x = \mathrm{Re}\, z(e^{i\phi}, t)$ in the vicinity of the points $x = 10,\ y = 0$ at times $t = 47,\ t = 50,\ t = 53,\ t = 56$ for two different values of the noise strength: (a) corresponds to $\kappa = 6$ and (b) corresponds to $\kappa = 16$. The widths of fjords are determined by the ratio $\nu/Q = 0.04$. The positions of points $\zeta_1(t) = z[1/\bar{\xi}_1(t), t]$ on the z plane can be considered as pointlike obstacles in the Hele-Shaw flow. By flowing around these points, the interface develops a variety of tiny fjords of water separating the fingers of oil on the microscale. The higher values of the noise strength generate the more fjorded interfaces. The boxed region in (a) shows the interface in the vicinity of the points $x = 10,\ y = 0$, magnified 20-fold and 200-fold correspondingly. Since the interface exhibits similar patterns on increasingly small scales, one can argue that the interface in the bottoms of fjords has a fractal structure.

fjords. The boxed region in Fig. 4(a) shows the interface in the vicinity of the points $x = 10,\ y = 0$, magnified 20-fold and 200-fold correspondingly. Since the interface exhibits similar patterns on increasingly small scales, one can argue that the interfaces in the bottoms of fjords have fractal structures.

A nontrivial relation between the auxiliary and the physical times (5) results in the reduction in amplitude of angular fluctuations of the fjord centerlines with time. This feature of the fjord's evolution can be already observed in Fig. 3. However, it is more instructive to consider the fjord's evolution on larger scales. In Fig. 5, we show the formation of the fjord's centerline for the noise strength $\kappa = 16$ generated

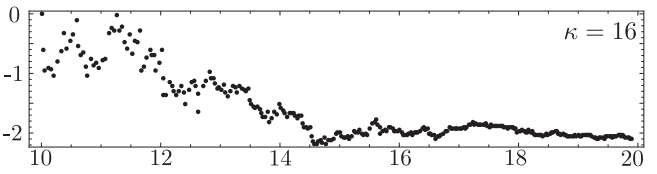

FIG. 5. We plot the fjord's centerline $y = \mathrm{Im}\, z[1/\bar{\xi}_1(t), t]$ vs $x = \mathrm{Re}\, z[1/\bar{\xi}_1(t), t]$, generated by stochastic dynamics of singularities of the conformal map (4) for $\kappa = 16$ during the first 4 s of the growth process. We see a fast reduction in the amplitude of angular fluctuations of the curve with time so that initially chaotic distribution of points quickly reduces to an almost smooth curve, thus, generating the well-known logarithmic solutions of the Hele-Shaw problem.

in the first 4 s of the stochastic growth process. We see that initially chaotic distribution of points quickly reduces to an almost smooth curve.

We conclude that the proposed stochastic growth model allows one to address the fractal properties of patterns at the bottoms of deep fjords where tiny fjords repeatedly merge together to form the larger ones (see Fig. 4). However, further elaboration of the model is required to explain the formation of fractal branched patterns on the macroscale: since the fjords' centerlines quickly become almost smooth curves, tip splitting and side branching of viscous fingers on the macroscale cannot be explained by the proposed model [see Fig. 2]. Note, however, that random fluctuations in pressure appear inevitably during the whole growth process, thus, producing various generations of fjords on the macroscale. This process manifests itself in the repeated events of tip splitting and side branching of viscous fingers (in this paper, we consider the time evolution of the only generation of fjords).

VI. CONCLUSION AND DISCUSSION

In this paper, we introduced and studied a self-consistent model of stochastic interface dynamics in the Hele-Show cell described by Eqs. (1), (2), and (4). Our initial motivation was to consider the effect of the short-distance regularization of the interface dynamics suggested by the aggregation model [7–9], which effectively makes the two-dimensional fluid compressible on the microscale, and, therefore, allows one to study *local* fluctuations of pressure in the vicinity of the moving interface. Let us briefly summarize the results.

We argued that dissipation of fluctuations in pressure results in the evolution of tiny initial perturbations at the interface into the patterns with well-developed fjords of oil separating fingers of water. The introduced model, in particular, explains a relevance of logarithmic solutions in the Hele-Shaw problem (on the large scale), and why these solutions are found to be in excellent agreement with the known experimental observations [15,16,29,30]. By using numerical simulations, we presented typical patterns generated by stochastic Laplacian growth (1), (2), and (4) in Figs. 2–5.

We also argued that the only stochastic dynamics of poles of the conformal map, consistent with the interpretation of martingales as conditioned statistical averages, is given by (4).

A role of the noise strength κ can be anticipated by using the following rough estimate. If to ignore the interaction between the poles, Eq. (4) takes the form:

$$d\ \ln\ \xi_k(t) = -\sigma\ dq_k(t) + i\, dW_k(t). \tag{24}$$

By using $\xi_k(t) = r_k(t)e^{i\varphi_k(t)}$, one can reduce the complex equation (24) to the following real equations:

$$d\ \ln\ r_k(t) = -\sigma\ dq_k(t), \quad d\varphi_k(t) = dW_k(t). \tag{25}$$

From the first equation, it follows that the poles move toward the origin regardless of the noise strength.[13] The second equation implies that the noise strength determines the angular spread of the points of the fjord's centerlines. Because of (5), the amplitude of angular fluctuations of the fjords' centerlines quickly reduces with time. These arguments are in excellent agreement with numerical simulations presented in Figs. 3–5. Thus, the proposed model of stochastic interface dynamics in the Hele-Shaw cell generates fractal patterns on the microscale where tiny fjords repeatedly merge together to form the large ones.

Although the introduced model provides a promising angle for understanding Laplacian growth, much remains to be done. Contrary to the conventional cutoff mechanisms, e.g., by means of the surface tension, the proposed model allows one to study *analytically* regularized interface dynamics in the Hele-Shaw cell, thus simplifying analysis of the problem. In particular, it becomes possible to consider some long-standing problems in Laplacian growth by means of novel analytical methods.

For example, it is instructive to revise the pattern selection problems, e.g., a selection for the Saffman-Taylor finger propagating in a long rectangular Hele-Shaw cell. Historically, the problem was addressed by including surface tension and applying the nontrivial WKB-like technique. We believe that Eqs. (1), (2), and (4) (after minor modifications due to rectangular geometry) allow one to study evolution of tiny perturbations at the initial flat front into the Saffman-Taylor finger occupying exactly $1/2$ of the channel width. The next step would be to consider the pattern selection problem in the so-called wedge geometry, which serves as a prototype (building block) for the whole growing structure since any fingerlike fragment of a moving interface can be considered as propagating in a virtual wedge geometry formed by centerlines of two fjords surrounding the finger.

The relation between the martingales and the conformal correlations functions also deserves further study. The correlation functions (7) [due to the transformation rules (6)] allow one to estimate a scaling of the harmonic measure $|w'(z,t)|$ in the bottoms of fjords. The main idea is to use a Coloumb gas formalism [21], which was previously applied to consider a harmonic measure of SLE curves [19]. However, coupling of the Gaussian free field to the growing domain runs into difficulties, which are beyond the scope of this paper, and will be considered in future publications.

We emphasize that the introduced model of stochastic interface dynamics generates fractal patterns on the *microscale* where tiny fjords repeatedly merge together. However, since the fjords center lines quickly become smooth curves (see Fig. 5), further elaboration of the model is required to explain the fractal patterns on the *macroscale*. One can argue that fluctuations in pressure inevitably appear during the whole growth process, thus, resulting in the tip splitting and side branching of viscous fingers. Therefore, the next important step is to study regularized Laplacian growth obtained by driving the interface dynamics (1), (2), and (4) with a compound random process producing fluctuations with time.[14]

Afterwards, it will become possible to attack derivation of a spectrum of fractal dimensions. The patterns typically generated in the Hele-Shaw flow have the same universal Hausdorff dimension $D_F = 1.71 \pm 0.01$, which is still out of analytic reach [32]. Although the fractal dimension in the bottoms of deep fjords can be anticipated from our results,[15] they cannot be used to explain the fractal spectrum of the whole interface because of the existence of different scales in the model. The patterns on the macroscale are developed by side branching and tip splitting of viscous fingers due to different fjords' generations. It is remarkable, however, that Laplacian growth generates *monofractals* [10]. This result implies a nontrivial relation between different scales of the model (probably, this connection can be addressed by renormalization group arguments) and will be considered in future publications.

ACKNOWLEDGMENT

The work is supported by Native towns, a social investment program of PJSC Gazprom Neft.

APPENDIX A: SHORT-DISTANCE REGULARIZATION OF LAPLACIAN GROWTH

A standard formulation of the Hele-Shaw problem is as follows [3]. The droplet of water D_t^+ is surrounded by a viscous fluid (oil) $D_t^- = \mathbb{C} \setminus D_t^+$, called D_t for simplicity. The velocity of viscous fluid in a thin gap between two parallel plates obeys Darcy's law $\mathbf{v} = -\nabla P$ (in scaled units) where the pressure $P(z)$ as a function of $z = x + iy$ satisfies the Laplace equation with a sink at infinity, i.e., $\nabla^2 P = 0$, and $P(z) = -Q\ \ln|z|$ as $z \to \infty$. If one neglects the surface tension, $P = 0$ at the interface between two fluids. The kinematic identity requires the normal interface velocity to be equal to the fluid velocity at the interface $v_n = -\partial_n P(\zeta),\ \zeta \in \partial D$, where ∂_n stands for the normal derivative at the boundary. Solutions to Laplace equation $\nabla^2 P = 0$ can be written in terms of Green's functions of the (external) Dirichlet boundary problem,[16] namely, $P(z,t) = QG_{D_t}(z,\infty)$. By using $G_{D_t}(z,\infty) = -\ln|w(z,t)|$,

[13] More precisely, $dq_k(t)$ depends on κ through $|z'(w,t)|$. This dependence, however, is insignificant in the limit $r(t) \to \infty$.

[14] A similar idea was previously implemented to describe the Loewner evolution with random branching curves [31].

[15] As we mentioned, the analytic analysis of this problem requires advanced field theoretical methods, which are beyond the scope of this paper.

[16] By definition, $G_D(z,z')$ is a harmonic function in D, except at $z = z'$, where $G_D(z,z')$ diverges as $\ln|z - z'|$ and $G_D(z,z') = 0$ at the boundary ∂D [33].

where $w(z,t)$ is a conformal map from the exterior of the domain D_t^+ to the exterior of the unit disk and computing the pressure gradient at the boundary, one determines the normal velocity of the interface,

$$v_n(\zeta,t) = Q|w'(\zeta,t)|, \quad \zeta \in \partial D_t. \tag{A1}$$

Equation (A1) describes two-dimensional free boundary dynamics of a viscous incompressible fluid, pushed out by another inviscid liquid or a gas. In terms of the conformal map $z(w,t)$, Eq. (A1) takes the form

$$\mathrm{Im}[\overline{\partial_t z(e^{i\phi},t)}\partial_\phi z(e^{i\phi},t)] = Q, \tag{A2}$$

which was intensely studied earlier and known to possess a rich integrable structure [3].

The idealized Laplacian growth problem (A2) is ill defined because initially smooth interfaces quickly evolve into fingerlike patterns, which develop cusp singularities at finite time [34]. Indeed, the Hele-Shaw dynamics (A2) of the n-fold perturbed unit circle,

$$z(e^{i\phi},t) = r(t)e^{i\phi} + a(t)e^{i(1-n)\phi} \tag{A3}$$

results in the fast growth of the perturbation $a(t) = a_0[r(t)]^{n-1}$, thus, evolving in the needlelike cusps.

On the other hand, there exists a family of explicit logarithmic solutions, which remain smooth for all times [11],

$$z(e^{i\phi},t) = r(t)e^{i\phi} + \sum_{k=1}^{N} \alpha_k \ln\left[\frac{e^{i\phi}}{a_k(t)} - 1\right], \tag{A4}$$

where $\sum_{k=1}^{N}\alpha_k = 0$ and $|a_k(t)| < 1$. Time dependence of $a_k(t)$ and $r(t)$ can be obtained from the equations,

$$\beta_k = z[1/\bar{a}_k(t),t] = \mathrm{const}, \quad 2\pi t = \mathcal{A}_t, \tag{A5}$$

where $\mathcal{A}_t = (1/2i)\oint_{|w|=1}\overline{z(w,t)}z'(w,t)dw$ is the area of the growing domain at time t. The logarithmic terms in (A4) have a clear geometric interpretation of oil fjords with parallel walls separating the fingers of water. These patterns are found to be in excellent agreement with some experiments [29,30] (see also Ref. [23] for a more general family of "multicut" solutions, which describe fjords with nonparallel walls).

The mentioned agreement between the logarithmic solutions and the experimentally observed patterns raises a natural question: *Why do the logarithmic (and multicut) solutions appear to be extremely important in the Hele-Shaw problem and describe the experimentally observed patterns?*

It was argued previously that these patterns can be understood as examples of the pattern formation in the regularized Hele-Shaw problem [9]. Let us briefly summarize the main results:

(i) The formation of cusps is forbidden: The regularization procedure suggests that the inviscid fluid (water) consists of particles with a minimal area $\hbar$, which serves as a short-distance cutoff curbing singularities of the fluid dynamics [7]. The growth process is generated by the aggregation of a large number $K \gg 1$ of uncorrelated Brownian particles of the size $\hbar$ issued from infinity and stuck to the interface per time unit [8].

(ii) Upon the short-distance regularization, the Hele-Shaw problem possesses a dimensional parameter, i.e., the particle size $\hbar$. Simple combinatorics allows one to study random distributions of the attached particles (per time unit), which have a clear geometrical interpretation as static fluctuations at the interface. Statistics of the fluctuations is described by Dyson's circular ensemble [9,35].

(iii) It is assumed that solutions to the regularized problem permit separation of scales in a form of a slow modulation of fast fluctuations (on a scale on the order of $\hbar$) at the boundary. The hydrodynamical evolution of the interface (1)–(3) can be obtained by averaging over the fast fluctuations [9].

APPENDIX B: LAPLACIAN GROWTH IN THE PRESENCE OF FLUCTUATIONS

Let us briefly review the growth process generated by the coupled equations (1)–(3). It can be *formally* represented as the idealized Laplacian growth problem with time-dependent oil sources. Indeed, from Eqs. (1) and (2), one obtains the effective pressure field, which drives the interface dynamics,

$$P(z,t) = (Q+\nu N)G_{D_t}(z,\infty) - \nu\sum_{k=1}^{N} G_{D_t}(z,\zeta_k), \tag{B1}$$

so that $\nabla^2 P = \nu\sum_{k=1}^{N}\delta^{(2)}(z-\zeta_k)$, where $\zeta_k(t) = z[1/\bar{\xi}_k(t),t]$ and $P = -Q\ln|z|$ as $z\to\infty$. Thus, the points $\zeta_k(t)$ can be considered as the positions of oil sources with rates ν. The motion of ξ_k's with time (3) results in the time evolution of ζ_k's inside the oil domain.

The emergence of these sources can be misleading because the only physical oil sink is located at infinity [from Eq. (B1), it also follows that the total growth rate is Q]. This apparent contradiction has the following resolution. The short-distance regularization suggested by the aggregation model effectively leads to a compressible liquid on a microscale due to a finite size and irregular shape of the particles. The incompressibility condition holds in the bulk, where $P = QG_{D_t}(z,\infty)$ but is violated in the vicinity of the boundary on a scale on the order of $\hbar$. Thus, tiny perturbations in pressure close to ∂D_t only formally can be attributed to the oil sources of the Hele-Show flow.

The violation of the incompressibility condition on the microscale allows one to introduce *local* fluctuations in pressure in the vicinity of the interface, which are forbidden in the idealized Hele-Show problem. Indeed, due to a continuity condition, small perturbations of the interface, e.g., Eq. (A3), result in variations of the pressure field in the viscous fluid. However, because of the incompressibility of oil, these variations are nonlocal and require to change the pressure field in the whole domain occupied by a viscous fluid.

Small perturbations of the initial smooth contour do not evolve in cusp singularities at the interface: Solutions to Eqs. (1)–(3), which are the time-dependent conformal maps $z(e^{i\phi},t)$ with the *dynamically generated* branch cuts inside the unit circle, describe the formation of oil (viscous fluid) fjords with nonparallel walls separating the fingers of water [9]. Thus, the logarithmic solutions (A4) naturally appear in the regularized Hele-Shaw problem.

Let $\xi_k^0 = \xi_k(t_0)$ be the coordinates, which determine the initial perturbation at the interface at time t_0. From Eqs. (1) and (2), it follows that the conformal map $z(w,t_0)$ has simple poles at ξ_k^0. The growth process, Eqs. (1)–(3), then implies

a splitting of these poles into the branch cuts $\tilde{\gamma}_k(t)$ $(t > t_0)$ with the time-dependent end points $\xi_k(t)$ and $\xi_k^{(0)}(t)$ so that $|\xi_k(t)| \to 0$ and $|\xi_k^0(t)| \to 1^-$ as $\tau(t) \to \infty$.[17] Tiny perturbations at the initial circle $z = r(t_0)e^{i\phi}$, similar to (A3), do not lead to the formation of cusps but evolve in the contour, which can be represented as a sum of Cauchy type integrals [9],

$$z(e^{i\phi}, t) = re^{i\phi} + u_0 - \sum_{k=1}^{N} \int_{\tilde{\gamma}_k(t)} \frac{\bar{\mathcal{P}}_k\{\bar{z}[1/\xi(t), t], t\}}{\xi - e^{i\phi}} \frac{d\xi}{2\pi i}, \tag{B2}$$

where $\mathcal{P}_k[z(1/\bar{\xi}, t), t]$ are the time-dependent Cachy densities on the cuts $\tilde{\gamma}_k(t)$ with the end points $\xi_k^0(t)$ and $\xi_k(t)$. The Cauchy densities are determined by the velocities of the end points $\zeta_k(t) = z[1/\bar{\xi}_k(t), t]$ on the z plane [see the discussion below Eq. (C1)]. In particular, the uniform motion of ζ_k's generates the fjords described by logarithmic solutions (A4).

APPENDIX C: THE SCHWARZ FUNCTION APPROACH

The Schwarz function provides an elegant geometrical interpretation of solutions to the Hele-Shaw problem. The Schwarz function $\mathcal{S}(z, t)$ for a smooth curve $\Gamma_t \subset \mathbb{C}$ is an analytic function in a striplike neighborhood of the curve such that $\bar{z} = \mathcal{S}(z, t)$ for $z \in \Gamma_t$ [36]. It can be decomposed in a sum of two functions $\mathcal{S}^+ = \sum_{k\geqslant 0} \mathcal{S}_k z^k$ and $\mathcal{S}^- = \sum_{k\geqslant 1} \mathcal{S}_{-k} z^{-k}$, that are regular in D_t^+ and D_t^-, respectively.[18] The idealized deterministic Laplacian growth (A2) implies that $\mathcal{S}^+(z, t)$ does not vary in time, thus, possessing an infinite number of conserved quantities $\mathcal{S}_k = \text{const}$ $(k > 0)$. A physical interpretation of this result is straightforward: The initial circle $z = r_0 e^{i\phi}$ continues to stay as the circle $z = r(t)e^{i\phi}$ with a growing radius $r(t)$.

In the *regularized* problem $\dot{\mathcal{S}}_k \neq \text{const}$ $(k > 0)$ but slowly decays with time. The Schwarz function $\mathcal{S}^+$ can be represented as a sum of Cauchy type integrals [9],

$$\mathcal{S}^+(z, t) = \mathcal{S}^+(z, 0) + 2\nu \sum_{k=1}^{N} \int_{\gamma_k(t)} \frac{\mathcal{P}_k(l)dl}{z - l}, \tag{C1}$$

where the integration contours $\gamma_k(t)$ are the trajectories of $\zeta_k(t)$ on the z plane. The Cauchy densities $\mathcal{P}_k(l) = 1/v_k(l)$ are determined by the velocities $v_k(l) = dl(t)/dt$ of the end points $\zeta_k(t)$.

In terms of the Schwarz function, the growth process (1), (2) reads [9]

$$\mathcal{S}^+(z, t_i) - \mathcal{S}^+(z, t_{i-1}) = \nu\, \Delta t \sum_{k=1}^{N} \frac{1}{z - \zeta_k(t_i)}. \tag{C2}$$

The interface dynamics, described by this equation, is similar to the idealized Hele-Show dynamics with N oil sources at the points $\zeta_k(t_i)$ and a sink at ∞ (see also Appendix B). Equation (C2) implies that logarithmic branch points $\zeta_k(t_j)$ $(0 \leqslant j < i)$ of the function $\mathcal{S}^+(z, t_{i-1})$ are integrals of motion,

$$\zeta_k(t_j) = z\big[1/\bar{\xi}_k^j(t_i), t_i\big] = \text{const} \quad (j < i), \tag{C3}$$

Solutions (B2) [or (C1)] to the regularized Laplacian growth problem Eqs. (1)–(3) have a clear geometrical interpretation (see Fig. 1):

(a) The branch cuts of the Schwarz function $\gamma_k(t)$, which coincide with the trajectories of ζ_k's inside the oil domain, are the centerlines of the dynamically generated oil fjords. Because of the interaction (3), the centerlines are typically curved.

(b) The walls of the fjords are not parallel but have nonzero opening angles determined by the velocities of the branch points $\zeta_k(t)$ of the Schwarz function.

[17] One can show that $\xi_k^0(t)$ approaches the unit circle $|\xi_k(t)| \to 1^-$ as $t \to \infty$ but never touches it [24].

[18] The coefficients $\mathcal{S}_{\pm k} = \mp \int_{D^\mp} z^{\mp k} d^2 z$ are the external and internal harmonic moments of the domain correspondingly.

[1] H. E. Stanley and N. Ostrowsky, *On Growth and Form*, Nato Science Series E (Springer, Amsterdam, 1986).

[2] P. Pelce and A. Libchaber, *Dynamics of Curved Fronts*, Perspectives in Physics (Academic, San Diego, 1988).

[3] D. Bensimon, L. P. Kadanoff, S. Liang, B. I. Shraiman, and C. Tang, Rev. Mod. Phys. **58**, 977 (1986).

[4] T. A. Witten and L. M. Sander, Phys. Rev. Lett. **47**, 1400 (1981).

[5] S. Richardson, J. Fluid Mech. **56**, 609 (1972).

[6] M. Mineev-Weinstein, P. B. Wiegmann, and A. Zabrodin, Phys. Rev. Lett. **84**, 5106 (2000).

[7] O. Agam, E. Bettelheim, P. Wiegmann, and A. Zabrodin, Phys. Rev. Lett. **88**, 236801 (2002).

[8] O. Alekseev and M. Mineev-Weinstein, Phys. Rev. E **94**, 060103(R) (2016).

[9] O. Alekseev, Phys. Rev. E **100**, 012129 (2019).

[10] T. C. Halsey, Phys. Today **53**(11), 36 (2000).

[11] M. B. Mineev-Weinstein and S. P. Dawson, Phys. Rev. E **50**, 24(R) (1994).

[12] K. Löwner, Math. Ann. **89**, 103 (1923).

[13] P. P. Kufarev, Rec. Math. [Mat. Sbornik] N.S. **13**, 87 (1941), in Russian.

[14] O. Schramm, Isr. J. Math. **118**, 221 (2000).

[15] E. Lajeunesse and Y. Couder, J. Fluid Mech. **419**, 125 (2000).

[16] L. Ristroph, M. Thrasher, M. B. Mineev-Weinstein, and H. L. Swinney, Phys. Rev. E **74**, 015201(R) (2006).

[17] I. Karatzas and S. Shreve, *Brownian Motion and Stochastic Calculus*, 2nd ed., Graduate Texts in Mathematics Vol. 113 (Springer, New York, 1998).

[18] M. Bauer, D. Bernard, and K. Kytölä, J. Stat. Phys. **120**, 1125 (2005).

[19] E. Bettelheim, I. Rushkin, I. A. Gruzberg, and P. Wiegmann, Phys. Rev. Lett. **95**, 170602 (2005).

[20] A. A. Belavin, A. M. Polyakov, and A. B. Zamolodchikov, Nucl. Phys. B **241**, 333 (1984).
[21] P. Francesco, P. Mathieu, and D. Sénéchal, *Conformal Field Theory*, Graduate Texts in Contemporary Physics (Springer, New York, 1997).
[22] M. Bauer and D. Bernard, Commun. Math. Phys. **239**, 493 (2003).
[23] A. Abanov, M. Mineev-Weinstein, and A. Zabrodin, Physica D **238**, 1787 (2009).
[24] S. P. Dawson and M. Mineev-Weinstein, Phys. Rev. E **57**, 3063 (1998).
[25] Y. Nakayama, Int. J. Mod. Phy. A **19**, 2771 (2004).
[26] M. Bauer and D. Bernard, Phys. Lett. B **557**, 309 (2003).
[27] A. Gamsa and J. Cardy, J. Phys. A **39**, 12983 (2006).
[28] D. Jasnow and C. Yeung, Phys. Rev. E **47**, 1087 (1993).
[29] L. Paterson, J. Fluid Mech. **113**, 513 (1981).
[30] L. M. Sander, P. Ramanlal, and E. Ben-Jacob, Phys. Rev. A **32**, 3160 (1985).
[31] F. Johansson and A. Sola, arXiv:0811.3857.
[32] O. Praud and H. L. Swinney, Phys. Rev. E **72**, 011406 (2005).
[33] R. Courant, *Dirichlet's Principle, Conformal Mapping, and Minimal Surfaces* (Springer, New York, 1950).
[34] B. Shraiman and D. Bensimon, Phys. Rev. A **30**, 2840 (1984).
[35] O. Alekseev and M. Mineev-Weinstein, J. Stat. Phys. **168**, 68 (2017).
[36] P. J. Davis, *The Schwarz Function and Its Applications*, The Carus Mathematical Monographs Vol. 17 (Mathematical Association of America, Buffalo, NY, 1974).